Journal of Colloid and Interface Science **230,** 420–431 (2000)
doi:10.1006/jcis.2000.7106, available online at http://www.idealibrary.com on IDEAL®

Wetting Study of Hydrophobic Membranes via Liquid Entry Pressure Measurements with Aqueous Alcohol Solutions

M. C. García-Payo,[1] M. A. Izquierdo-Gil, and C. Fernández-Pineda

Departamento de Física Aplicada I, Facultad de Ciencias Físicas, Universidad Complutense, 28040 Madrid, Spain

Received March 29, 2000; accepted July 17, 2000

A new concept of liquid entry pressure measurements is applied to study the hydrophobicity of microporous membranes for aqueous alcohol solutions. The effects of alcohol concentration, type of alcohol, and temperature on liquid entry pressure of the membrane have been studied. Two theoretical equations for the determination of membrane pore size have been proposed. The former equation was developed taking into account the deviation from the Laplace–Young equation due to the membrane structure by means of the structure angle. The latter equation was established considering only the range of alcohol concentration in which the dispersion component of liquid surface tension remains practically constant. Hydrophobicity has been expressed in terms of wetting surface tension, γ_L^w. Based on these measurements, the maximum concentration before the spontaneous wetting occurs would be predicted.

Key Words: **wetting; liquid entry pressure; microporous and hydrophobic membranes; aqueous alcohol solutions.**

1. INTRODUCTION

In several membrane processes, the choice of membrane is based on the pore size of the material. However, for separation of organic solutes from aqueous solutions in membrane processes (1, 2), or for explaining fouling phenomena (3), this requirement is not sufficient. In fact, for membrane distillation, which is a separation process of liquid mixtures through porous hydrophobic membranes (4, 5), the pore size requirement is not sufficient. The main requirement in this process is that the membrane must not be wetted by liquid mixture. Interactions of liquid solutions with the membrane are an important parameter in these processes; therefore, in addition to the pore size, the hydrophobicity of the membrane must be known.

Different methods have been reported in the literature to determine the hydrophobicity of the membrane and its pore size. The pore size and its distribution can be known by the traditional methods such as mercury porosimetry, scanning electron microscopy, and the bubble point method (6) or by biliquid permporometry, thermoporometry (7), or the sticking bubble technique (8). From analysis of permeate flow as a function of pressure drop, the pore size distribution can also be obtained (9, 10). Hydrophobic porous membranes do not permit the liquid transfer until a certain pressure difference is exceeded. The liquid entry pressure (LEP) is defined as the pressure difference from which the liquid penetrates into the pores of the hydrophobic membrane (11). This critical pressure difference is correlated to the interfacial tension, the contact angle of the liquid on the surface, and the size and shape of membrane pores.

The liquid entry pressure is greatly important in membrane distillation processes because the liquid–vapor interfaces are formed at the pore entrance of the membrane and the permeant is transported as a vapor through the pores of the membrane. The membrane is just a barrier between two nonwettable liquids and the separation performance is predominantly determined by the liquid–vapor equilibrium. Solutions of inorganic solutes in water have surface tensions greater than water surface tension (72 mN/m), so the liquid does not penetrate into the membrane pores. However, the surface tension, γ_L, decreases sharply when solutions contain organic solutes in water and if the concentration of organic solute becomes sufficiently high to exceed a certain critical value, spontaneous wetting of membrane occurs. Thus, the ranges of pressure difference, concentration, and temperature allowable in these processes can be determined from LEP measurements. Additionally, the LEP only takes into account pores that connect both ends of the membrane (which are called active pores), because the liquid cannot pass through pores with a blocked end (inactive pores). However, other methods such as permporometry or mercury porosimetry do not discern between active and inactive pores. Since the mass transfer in membrane distillation processes takes place as vapors through the active pores, the hydrophobicity of the membrane and its active pore size can be determined by LEP measurements. Another advantage of the LEP technique is that it can be measured under conditions similar to those normally used in membrane processes.

In previous experiments, we observed that the LEP was not dependent on the solution's concentration only, but also on the temperature (12). Therefore, we have studied the influence of the temperature and the solution concentration on the LEP, for several types of membranes and pore sizes. Additionally, other characteristic parameters of porous membranes such as the wetting surface tension, the maximum pore radius, and the structure

[1] To whom correspondence should be addressed.

0021-9797/00 $35.00

angle of the membrane will be estimated from LEP and contact angle measurements.

2. THEORY

The pressure difference at the liquid–vapor interface is expressed according to the Laplace-Young equation (1, 9, 10, 13), supposing uniform cylindrical pores and sufficiently small so that the curvature radius can be assumed to be constant. However, most of the membranes do not have cylindrical pores. Some membranes have a fibrous structure and the pores are the irregular spaces that remain between adjacent fibers. In other membranes, the pores are holes in a spongy structure and they tend to suffer direction changes, crossing between them. Franken *et al.* (1) introduced a geometry coefficient of the pore, B, which includes the irregularities of the pores ($B = 1$ for cylindrical pores and $0 < B < 1$ for no cylindrical pores). Kim and Harriott (13) studied a model for membranes with no cylindrical pores. They supposed that the membrane structure is as a reticular fiber structure, which is closer to real pores than the capillary uniform model, and deduced an equation similar to the Laplace–Young equation,

$$\Delta P = -\frac{2\gamma_L}{r}\cos\theta_{ef}, \qquad [1]$$

where ΔP is the pressure difference at liquid–vapor interface, γ_L is the liquid–vapor surface tension, θ_{ef} is the effective contact angle, and r is the pore radius, which is defined as half of the mean distance between fibers. θ_{ef} can be expressed in terms of contact angle, θ, and always $\theta_{ef} > \theta$.

If the geometry of the pore is axially irregular, a structure angle, α, may be defined as the angle between a pore wall element and the normal to the membrane surface in the axial direction, as shown in Fig. 1. The force due to the pressure difference across interface will be equal to the surface force so that the pressure difference at the interface can be written as (14)

$$\Delta P = -\frac{2\gamma_L}{r}\frac{\cos(\theta_A - \alpha)}{1 + \frac{R}{r}(1 - \cos\alpha)}, \qquad [2]$$

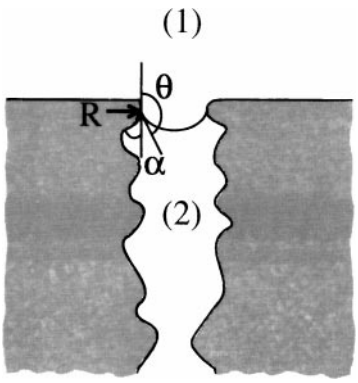

FIG. 1. Interface in an irregular pore of hydrophobic membrane. (1) Liquid phase and (2) gas phase.

where r is the mean pore radius, θ_A is the advancing contact angle, R is the mean curvature radius of pore wall element, and α is the average α since its value may change along the pore. The parameter R/r reflects the relative curvature of the membrane pore structure. Larger values of R/r correspond to rounder edged pores.

The LEP is the minimum value of ΔP at which the liquid penetrates into the largest pores of the membrane. This minimum value of ΔP occurs at the narrowest constriction when the structure angle reaches a maximum negative value. Therefore, if Eq. [2] is differentiated with respect to α and its derivative is equated to zero, it yields

$$\sin(\theta_A - \alpha) = \frac{R/r\,\sin\theta_A}{1 + R/r} \equiv \xi, \qquad [3]$$

and the minimum pressure difference can be estimated as

$$\mathrm{LEP} = -\frac{2\gamma_L}{r_{max}}\frac{\cos(\arcsin(\xi))}{\left[1 + 2\frac{R}{r}\sin^2\left(\frac{\theta_A}{2} - \frac{\arcsin(\xi)}{2}\right)\right]}. \qquad [4]$$

The r_{max} and R/r values can be estimated using experimental results of LEP, γ_L, and θ_A by nonlinear fit, or by minimizing a given function, χ^2, as it will be indicated below. The maximum structure angle, α_{max}, can be obtained using Eq. [2] and the estimated r_{max} and R/r values as explained later.

On the other hand, a distilled water droplet on a hydrophobic surface has a contact angle greater than 90°. If organic solutes are dissolved in water, the liquid surface tension will decrease, and consequently, the contact angle θ will decrease. When $\theta \lesssim 90°$ the liquid will penetrate into the membrane pores. The mechanical equilibrium state of a membrane–liquid–air system can be described by the Young equation as (15)

$$\gamma_L\cos\theta_{ef} = \gamma_S - \gamma_{SL}, \qquad [5]$$

where θ_{ef} is the effective contact angle of liquid on the membrane, γ is the surface tension, and the subscripts L, S, and SL refer to liquid–vapor, solid–vapor, and solid–liquid interfaces, respectively. If the roughness of the membrane surface is assumed to be equal to the roughness inside the pores, and if the pressure has no effect on contact angle, then the effective contact angle on the membrane pores can be approximated to the advancing contact angle on the membrane surface.

For polar or hydrogen bonding liquids (such as aqueous alcohol solutions) on nonpolar solids with low energy surfaces (such as PVDF or PTFE membranes), it can be supposed that the Van der Waals dispersion forces act between the liquid and solid phases only (16). Therefore, the interfacial tension between solid and liquid phases is given by

$$\gamma_{SL} = \gamma_S + \gamma_L - 2\sqrt{\gamma_S^d\gamma_L^d}, \qquad [6]$$

where γ_S^d and γ_L^d are the dispersion components of surface

tension of the solid and the liquid, respectively. The term $2\sqrt{\gamma_S^d\gamma_L^d}$ means dispersion components of the work of adhesion of a liquid to a solid surface. Substituting for γ_{SL} from Eq. [6] into Eq. [5] yields

$$\gamma_L \cos\theta = -\gamma_L + 2\sqrt{\gamma_S^d\gamma_L^d}. \qquad [7]$$

This equation is similar to Good–Girafalco–Fowkes–Young equation if the reduction in surface energy of the solid resulting from adsorption of vapor from liquid, π_S, and the reduction in surface energy of the liquid resulting from adsorption of a film of solid material from the solid, π_L, are considered negligible (17). For the case of PVDF and PTFE membranes, the surface energies are very low and it is expected that a strong interaction between the liquid and the solid exists (15, 16). Taking Eq. [1] into account, Eq. [7] can be solved yielding an equation that relates the liquid entry pressure with the liquid surface tension, the maximum pore radius, and the dispersion components of surface tension of the liquid and the solid:

$$\mathrm{LEP} = \frac{2}{r_{max}}\left(\gamma_L - 2\sqrt{\gamma_S^d\gamma_L^d}\right). \qquad [8]$$

For polar liquids, $\sqrt{\gamma_S^d\gamma_L^d}$ is not a constant. The dispersion component of surface tension of the solid, γ_S^d, is equal to γ_S, γ_S being almost constant, while γ_L^d varies with alcohol concentration until reaching a certain concentration value, from which the dispersion component of surface tension of the solution remains practically constant (18). If γ_L^d is constant, then $2\sqrt{\gamma_S^d\gamma_L^d} = \mathrm{cte} \stackrel{\mathrm{def}}{=} \gamma_L^W$, which we will denote as the wetting surface tension. Therefore, in the case of aqueous alcohol solutions, if it is considered the range of alcohol concentrations where γ_L^d remains practically constant only, Eq. [8] can be simplified as

$$\mathrm{LEP} = \frac{2}{r_{max}}\left(\gamma_L - \gamma_L^w\right) \qquad \begin{pmatrix}\gamma_S^d \simeq \mathrm{cte}\\ \gamma_L^d \simeq \mathrm{cte}\end{pmatrix}. \qquad [9]$$

Note that the wetting surface tension is the value of the surface tension when LEP is equal to zero, so it corresponds to the highest value of the surface tension of all the solutions that wet spontaneously the membrane pores. The wetting surface tension can be estimated from linear fit of liquid entry pressure versus surface tension for different alcohol concentrations. In addition, a maximum pore radius value can be estimated from its slope.

3. MATERIALS AND METHODS

Two different experimental techniques have been used in this work. The liquid entry pressure has been measured for different membranes, solutions, and temperatures, and additionally, advancing contact angle measurements have been performed in some cases.

Two commercial types of flat sheet hydrophobic membranes were used: one sort of PVDF provided by Millipore, which had 0.22 μm (PVDF22) and 0.45 μm (PVDF45) pore sizes, and the other of PTFE provided by Gore, which had 0.20 and 0.45 μm pore sizes, without support, (PTFE20 and PTFE45, respectively), and an additional one supported by a polypropylene net with 0.20 μm pore size (PTFS20). Membranes were tested as received without any pretreatment. Distilled water and aqueous solutions of methanol, ethanol, isopropanol, or *tert*-buthanol at different concentrations were used. The aqueous solutions used in this work were freshly prepared from analytical grade alcohol and distilled water. All the liquids were degassed using an ultrasonic bath for 10 min.

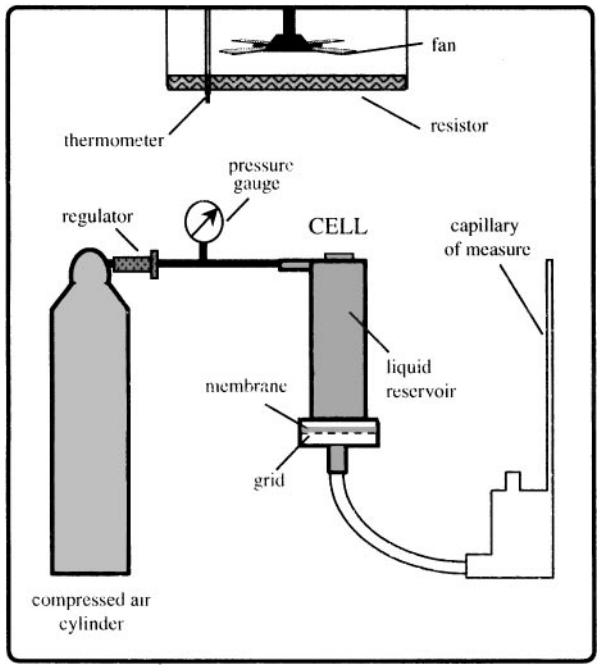

FIG. 2. Experimental apparatus for liquid entry pressure measurements.

The experimental apparatus used to measure liquid entry pressure is shown in Fig. 2. The membrane cell was a stainless steel filter holder with a reservoir of 200 ml supplied by Sartorius. The wetted membrane area was 13 cm^2. Compressed air was used to generate the applied pressure, which was controlled by a precision pressure regulator. The applied pressure relative to the atmospheric pressure was measured with a digital pressure gauge (range, 0 to 6 bar; supplied by Wika) connected to the upper part of the membrane cell. A small vessel provided with a capillary of 1 mm inner diameter was placed at the outlet of the cell in order to observe the continuous liquid flow, according to the procedure described in (11). The experimental apparatus was introduced in an air thermostat to measure at different temperatures. The measurement procedure was as follows: the measurement capillary and the bottom part of the membrane cell were filled with distilled water or an aqueous alcohol solution as permeating liquid. A dry membrane was placed on the grid and the cell reservoir was filled with the same liquid. When the equilibrium temperature was reached, the pressure

difference was increased slowly and stepwise by adjusting the pressure regulator. The flow rate was obtained by measuring the position of the liquid meniscus in the capillary as a function of time using a cathetometer. The LEP value was taken as the applied pressure difference at which the liquid flow was continuous. The LEP was measured on three different samples of the same membrane for each concentration and temperature. A fourth sample was measured when there was a significant dispersion of the results. The LEP was obtained from the mean value. The temperatures were 20°C (ambient temperature) and 25, 40, and 50°C (in the air thermostat).

Advancing contact angles were measured with the sessile drop method using distilled water and aqueous solutions of several alcohols at different concentrations. All the experiments were carried out at 25°C. A piece of membrane (of 2×2 cm^2) was placed on a platform situated in a chamber that was closed later in order to minimize evaporation, and the drop was observed through a window. The membrane was previously mounted on a 1-mm-thick PTFE frame in order to avoid the possible influence of the platform on the drop. The drop volume, 10–15 μl, was controlled by a microsyringe. The contact angles were calculated from a digital video image of the drop on the membrane using an image-processing program, which allowed the estimation of the contact angle from the height and the width of the drop. The value of contact angle was averaged over at least six drops for each membrane and alcohol concentration. Each measurement lasted less than 1 min in order to minimize the effects of variation of the contact angle versus time and of evaporation of the liquids used. It was experimentally found that the contact angle remained constant within this time. Additionally, the dependence of contact angle on drop size was neglected since Drelich *et al.* (19) observed that the contact angle/drop size relationship for rough surfaces does not affect significantly the advancing contact angle when the drop base diameter is varied from 1 to 7 mm.

4. RESULTS AND DISCUSSION

4.1. Liquid Entry Pressure Measurements

Figure 3 shows an example of the flow rate observed in the capillary as a function of applied pressure difference for different isopropanol solutions in water as permeating liquids and PTFS20 membranes. It can be seen that the flow rate increases very sharply as the pressure difference across the membrane is increased beyond a minimum value or LEP. It is also worth noting that for the same flow rate the pressure difference decreased as alcohol concentration increased and that the slope of flow rate versus pressure difference tends to decrease as alcohol concentration decreases, being observed a more pronounced decrease for distilled water. All the experimental data were fitted to the best-fit empirical equation:

$$\frac{F}{\Delta P} = \frac{p_{\max}}{1 + \exp(-b(\Delta P - \Delta P_0))}, \qquad [10]$$

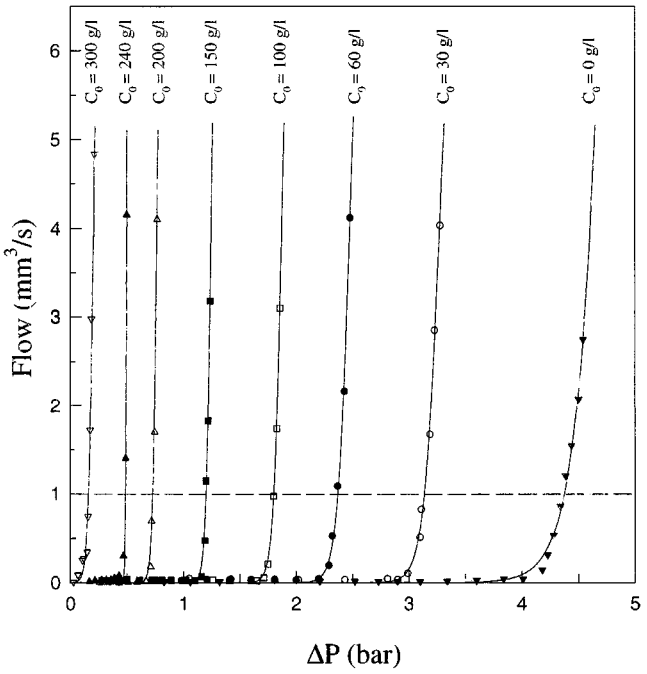

FIG. 3. Flow observed in the capillary as a function of the applied pressure difference for different isopropanol concentration in aqueous solutions at $t =$ 25°C. PTFS20 membranes. Solid lines represent the fits of the experimental data to Eq. [10].

where $F/\Delta P$ is defined as the liquid permeability and b, $p_{\max}$, and ΔP_0 are fitting parameters. $p_{\max}$ represents the maximum liquid permeability and ΔP_0 corresponds to the pressure difference when $F/\Delta P = p_{\max}/2$.

It is well known that when the pressure difference is increased beyond the minimum pressure difference, $\Delta P_{\min}$, the largest pores become wetted with the nonwetting liquid, and successively smaller pores become wetted as the pressure difference is further increased. When all the membrane pores are wetted, subsequent increases in pressure difference result in linear increases in flow rate, according to Darcy's law (9, 10). Exact determination of the liquid entry pressure, or $\Delta P_{\min}$, proved to be difficult. Additionally, with our experimental data Darcy's behavior was not reached (compare Fig. 3 with Fig. 4), so the value of the fitting parameter $p_{\max}$ was determined with a high uncertainty. Consequently, the LEP value was arbitrarily chosen as the pressure difference at which the flow rate observed in the capillary was equal to 1 mm^3/s, which assured that the liquid had penetrated into the membrane pores. Thus, errors due to processes of the membrane becoming convex and/or system expansion were also minimized.

Some complementary measurements were performed with higher flow values, so that Darcy's behavior was reached. From these measurements, it was possible to check the accuracy of the chosen LEP criterion. Several mass flux measurements versus applied pressure difference were carried out by weighting the liquid flow with a mass balance. PVDF22, PVDF45, and PTFE20 membranes were used at 25 and 40°C for distilled water

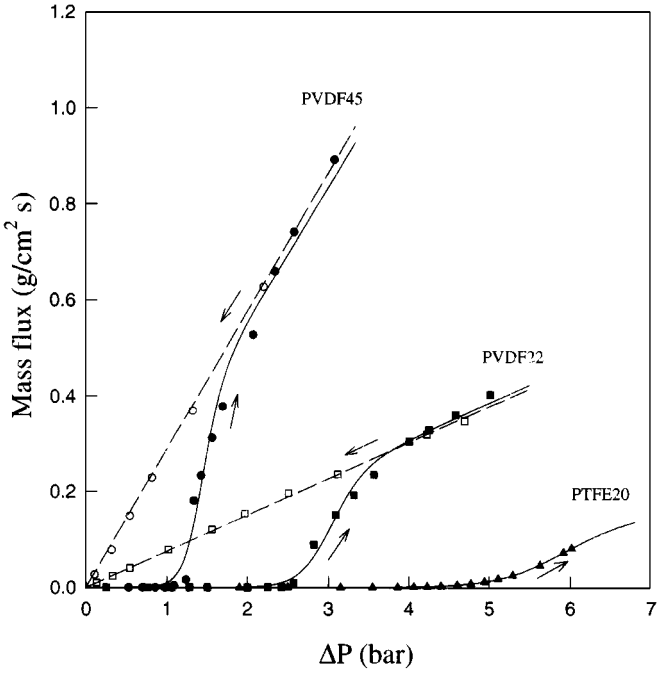

FIG. 4. Distilled water mass flux through membrane pores versus applied pressure difference for several membranes at $t = 25°C$. The filled symbols are values obtained with ascending ΔP, while the open symbols are values obtained with descending ΔP. Solid lines represent the fits of the experimental data to Eq. [10], and dashed lines represent Darcy's fits.

and aqueous isopropanol solutions at different concentrations. These nonwetting liquids were pressurized by compressed air in a high-pressure tank of stainless steel, and were supplied from it. Mass fluxes were measured with ascending ΔP until no increment of the mass flux versus applied pressure difference was detected. At this point, the applied pressure difference was decreased stepwise in order to observe the linear dependence on pressure difference when all the pores are wetted. Figure 4 shows the measured mass fluxes as a function of the applied pressure difference using distilled water as nonwetting liquid at 25°C. As can be seen in Fig. 4, the mass fluxes increase rapidly as the applied pressure difference is slightly increased more than the $\Delta P_{\min}$ value. In addition, the mass fluxes measured with descending ΔP show an excellent linear behavior, with larger slope as membrane pore size increases. This linear behavior is not observed for PTFE20 membrane because the pressure difference could not be increased beyond 6 bar due to the experimental limitations. Effect of membrane type on liquid permeability, $F/\Delta P$, is shown in Fig. 5. PTFE20 and PVDF22 membranes were used with an aqueous solution of 9 wt% isopropanol at $t = 40°C$ as nonwetting liquid. The filled symbols are values obtained with ascending ΔP, while the open symbols are values obtained with descending ΔP. A well-known linear behavior of mass fluxes for descending ΔP is also observed. The maximum liquid permeability, $p_{\max}$, for PVDF22 membranes is greater than that for PTFE20 membranes. In Figs. 4 and 5, the solid lines represent the fits of the experimental data to Eq. [10]. The correlation coefficients were greater than 0.99 for at least 16 points, and the experimental data were reproducible.

In order to check the LEP value criterion, some estimations were carried out. For the worst case (PTFS20 membrane and distilled water as testing liquid, see Fig. 3), the difference between the LEP value chosen and the ΔP value (for flow rate = 0.1 mm^3/s) was determined to be lower than 0.2 bar, which was included within experimental errors. It must also be pointed out that the error in flow rate was estimated to be about 0.2 mm^3/s. On the other hand, a flow rate of 1 mm^3/s (measured by means of the capillary) corresponds to a mass flux of the order of 7×10^{-5} g/cm^2 s for our experimental device. This mass flux can be considered negligible if the mass flux curves (measured by weighting) are taken into account, since the minimum mass flux observed is in the order of 1×10^{-3} g/cm^2 s (Figs. 4 and 5). It is also worth noting that the mass flux for $\Delta P_{\max}$ is in the order of 1×10^{-1} g/cm^2 s for the worst case. Therefore, it can be concluded from these estimations that the chosen LEP value is in a good agreement with the $\Delta P_{\min}$ value if the experimental errors are taken into account.

Figure 6 shows the liquid entry pressure versus alcohol concentration for aqueous solutions of ethanol or isopropanol. This set of experiments was carried out with PVDF22 and PVDF45 membranes at ambient temperature (≅20°C). It must be pointed out that LEP values for aqueous ethanol solutions are greater than LEP values for isopropanol solutions at same alcohol concentration. All the plots of LEP as a function of alcohol

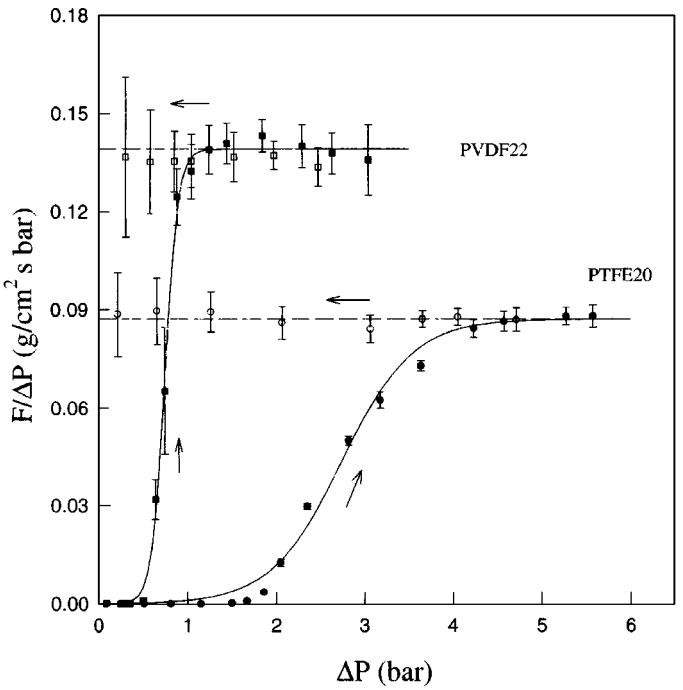

FIG. 5. Effect of membrane type on liquid permeability, $F/\Delta P$. PTFE20 and PVDF22 membranes, 9 wt% aqueous isopropanol solution as permeating liquid at $t = 40°C$. Filled symbols are values obtained with ascending ΔP, while open symbols are values obtained with descending ΔP. Solid lines represent the fits of the experimental data to Eq. [10], and dashed lines represent Darcy's fits.

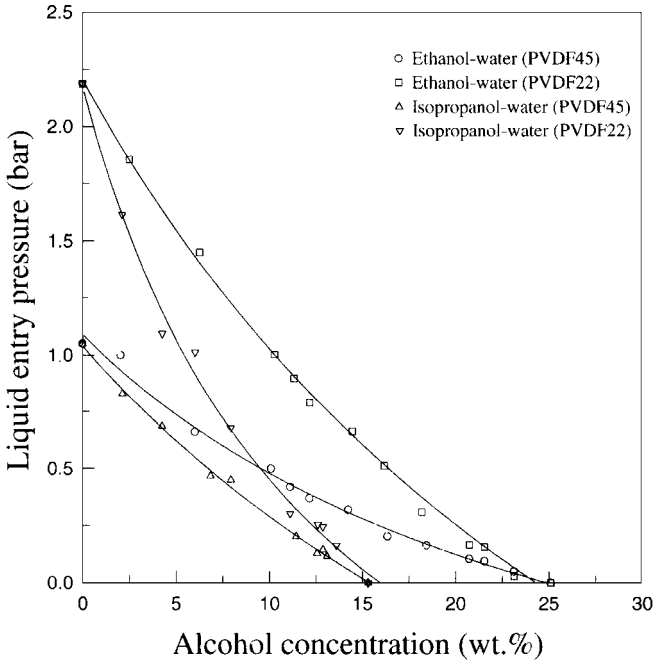

FIG. 6. Effect of membrane pore size and type of alcohol on liquid entry pressure, LEP. PVDF22 and PVDF45 membranes at $t \cong 20°C$. Solid lines represent the fits of the experimental data to Eq. [11].

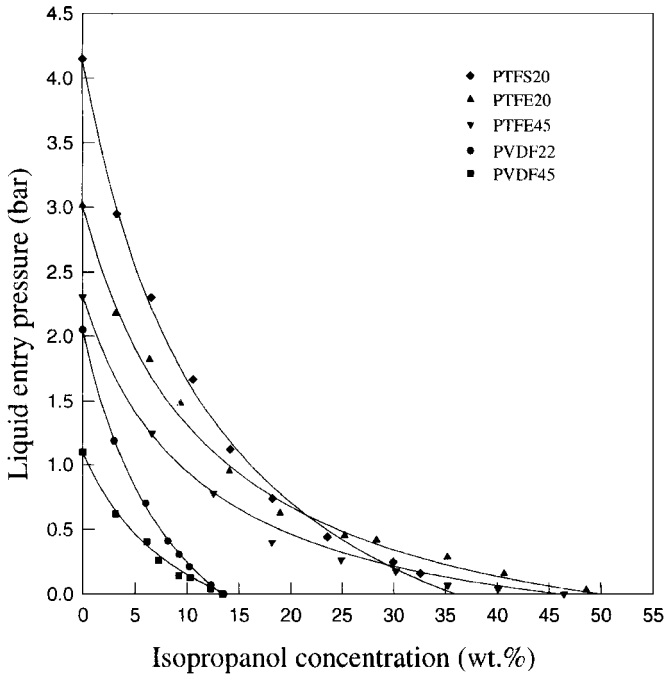

FIG. 7. Effect of membrane type on LEP. Aqueous isopropanol solutions at $t = 40°C$. Solid lines represent the fits of the experimental data to Eq. [11].

concentration for different temperatures, membranes, and alcohol types have been fitted to the best-fit empirical equation,

$$\mathrm{LEP} = \mathrm{LEP_W} - \frac{B \cdot c}{A + c}, \qquad [11]$$

where A, B, and $\mathrm{LEP_W}$ are fitting parameters. LEPw represents the distilled water entry pressure, and c is the alcohol concentration in percentage by weight. As seen in Fig. 6, excellent fits were achieved, obtaining correlation coefficients greater than 0.992 for at least 10 points.

The dependence of LEP on membrane type is shown in Fig. 7. Aqueous solutions of different isopropanol concentrations were used at $t = 40°C$. It is clearly observed that the LEP values obtained for PTFE membranes are greater than those for PVDF membranes. At a given isopropanol concentration, the LEP values for PTFE and PVDF membranes increase as the membrane pore size decreases. Both trends have also been observed for the different types of alcohol and temperatures studied in this work.

The wetting concentration, $c^{\mathrm{w}}_{\mathrm{exp}}$, is defined as the concentration when the LEP value is equal to zero and it corresponds to the lowest concentration of all the solutions that penetrate spontaneously into the membrane pores. The value of $c^{\mathrm{w}}_{\mathrm{exp}}$ can be calculated empirically from the fitting parameters of Eq. [11]. Such fitting parameters, $\mathrm{LEP_W}$, A, and B, as well as the values of $c^{\mathrm{w}}_{\mathrm{exp}}$ for different membranes and temperatures are summarized in Table 1. As can be seen in Figs. 6 and 7 and Table 1, the curves of LEP versus alcohol concentration intercept on the concentration axis in the neighborhood of a common value for the same type of membrane and alcohol. These results suggest that the studied membranes would become hydrophilic for a value of the concentration that is independent of the membrane pore size. For instance, the value of $c^{\mathrm{w}}_{\mathrm{exp}}$ was found to be 13–14 (±3) wt% of isopropanol for PVDF membranes at 40°C, and $c^{\mathrm{w}}_{\mathrm{exp}}$ varied from 46 to 49 (±6) wt% of isopropanol for PTFE membranes without support at 40°C.

The effect of the PP support of the PTFE membrane on liquid entry pressure was also studied. The $\mathrm{LEP_W}$ value for PTFS20 membrane is greater than that for the similar membrane without PP support (PTFE20), as shown in Fig. 7. However, from a given isopropanol concentration onward, the curve of LEP versus isopropanol concentration for PTFS20 membrane cuts those for PTFE20 and PTFE45 membranes, becoming hydrophilic at lower concentration than those for PTFE membranes without PP support. Additionally, an asymmetrical behavior for PTFS20

TABLE 1
Results of the Fit to Eq. [11] of the Experimental Data (Together with Their Standard Errors)

Membrane	t (°C)	$\mathrm{LEP_W}$ (bar)	A (wt%)	B (bar)	$c^{\mathrm{w}}_{\mathrm{exp}}$ (wt%)
PVDF22	25	2.17 (±0.02)	10.1 (±0.7)	3.6 (±0.1)	15 (±2)
	40	2.05 (±0.02)	9.2 (±0.5)	3.46 (±0.08)	13 (±2)
	50	1.91 (±0.03)	9.7 (±1.1)	3.4 (±0.2)	12 (±2)
PVDF45	40	1.10 (±0.03)	10 (±2)	1.89 (±0.14)	14 (±4)
PTFE20	40	3.01 (±0.07)	12.2 (±1.4)	3.74 (±0.15)	49 (±7)
PTFE45	40	2.32 (±0.05)	10.7 (±1.0)	2.90 (±0.08)	46 (±5)
PTFS20	40	4.15 (±0.07)	12.6 (±1.2)	5.6 (±0.2)	36 (±2)

Note. Aqueous isopropanol solutions for different membranes and temperatures.

membrane was observed. The LEP_W value was measured by placing the PTFE membrane side into contact with the grid, and applying pressure at the PP side at 40°C. In this configuration, the value of LEP_W was about 10 times less than the value of LEP_W measured by applying pressure at the PTFE side at the same temperature (from 4.25 ± 0.05 to 0.44 ± 0.07 bar). Moreover, PP support was separated from PTFE side and a hydrophilic behavior was observed due to the large pore size of the PP support (approximately 50 μm). Therefore, we think that the coupling between both materials would give rise to this asymmetrical behavior, being favored the flow in one way.

In order to study the effects of alcohol type on LEP, several sets of experiments were carried out for aqueous solutions of methanol, ethanol, isopropanol, or *tert*-buthanol at different alcohol concentrations. PVDF22 and PTFE20 membranes were used at 25 and 40°C. At a given alcohol concentration, the plots shown in Figs. 8 and 9 indicate that the LEP value for aqueous methanol solution is greater than the LEP value for ethanol solution, and the latter is greater than that for isopropanol solution. In the case of PTFE20 membranes, the lowest LEP value corresponds to aqueous *tert*-buthanol solutions. Wetting concentrations obtained for these membranes and alcohols are listed in Table 2. It is worth noting that the wetting concentration was always significantly higher for PTFE membranes than the wetting concentration obtained for PVDF membranes under same experimental conditions.

The effect of temperature on liquid entry pressure was also investigated. The data shown in Fig. 10 indicate that the LEP values tend to decrease with increasing temperature. This behavior is observed for PVDF and PTFE membranes as it can be inferred from the data listed in Tables 1 and 2.

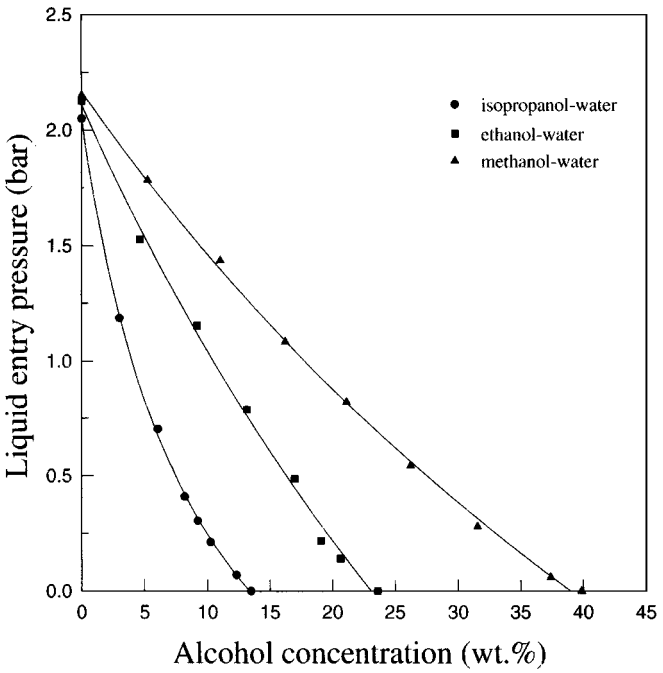

FIG. 8. Liquid entry pressure as a function of alcohol concentration for different alcohols in aqueous solutions. PVDF22 membranes at $t = 40$°C. Solid lines represent the fits of the experimental data to Eq. [11].

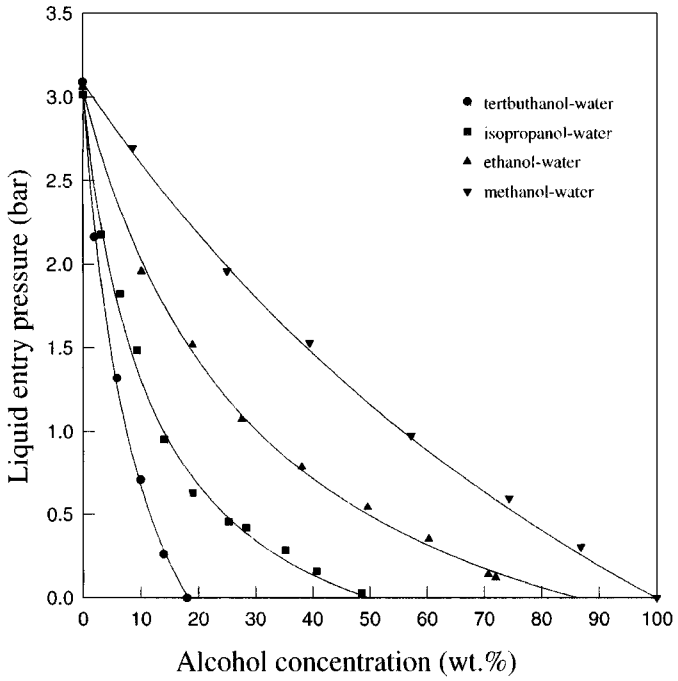

FIG. 9. Liquid entry pressure as a function of alcohol concentration for different alcohols in aqueous solutions. PTFE20 membranes at $t = 40$°C. Solid lines represent the fits of the experimental data to Eq. [11].

4.2. Contact Angle Measurements

Advancing contact angles of distilled water and aqueous solutions of different alcohols on several membranes were measured. Alcohol concentrations close to the wetting concentration for each alcohol and membrane were used. The mean values of

TABLE 2
Wetting Concentration, c^w_{exp}, Obtained from the Fit to Eq. [11] of the Experimental Data for Different Membranes and Temperatures

Membrane	t (°C)	Alcohol	c^w_{exp} (wt%)
PVDF22	40	Methanol	39 (±8)
	40	Ethanol	23 (±7)
	40	Isopropanol	13 (±2)
PTFE20	40	Methanol	100 (±19)
	40	Ethanol	85 (±9)
	40	Isopropanol	49 (±7)
	40	*tert*-Buthanol	18 (±3)
PTFE20	25	Methanol	>100[a] (±20)
	25	Ethanol	86 (±6)
	25	Isopropanol	54 (±5)
	25	*tert*-Buthanol	22 (±2)

Note. The estimated standard errors are indicated in parentheses.
[a] Note that pure methanol does not wet the membrane.

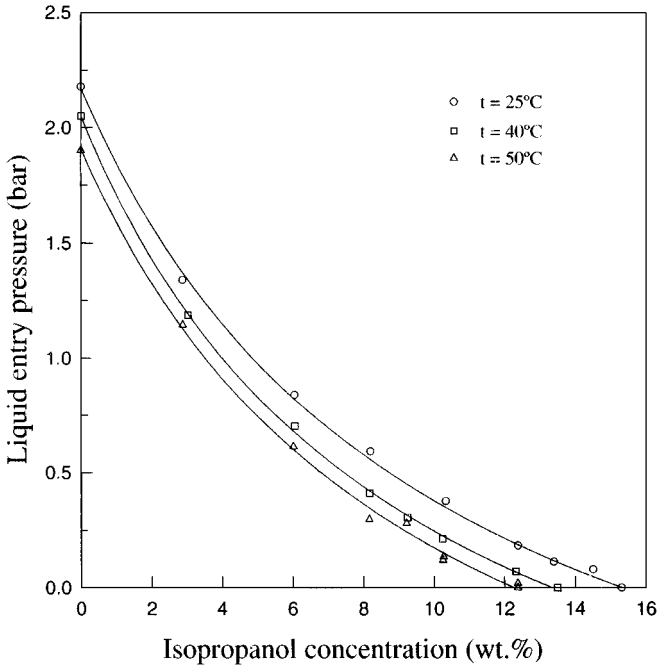

FIG. 10. Effect of temperature on LEP. Aqueous isopropanol solutions and PVDF22 membranes. Solid lines represent the fits of the experimental data to Eq. [11].

contact angles obtained for each type of alcohol and membrane are summarized in Table 3. It can be seen that the values of contact angle for distilled water on PTFE membranes are greater than those on PVDF membranes. It is also interesting to note that the contact angles for distilled water tend to be independent of membrane pore size, even if the membrane is supported or not (the contact angles for PTFS20 membranes were measured on the PTFE side). Mean values of θ for distilled water were estimated to be $111 \pm 3^\circ$ on PVDF membranes and $123 \pm 2^\circ$ on PTFE membranes. Additionally, a visual inspection of data appearing in Table 3 indicates that the contact angle decreases with increasing alcohol concentration, i.e., with decreasing liquid surface tension.

On the order hand, the membranes used in this work are not ideal smooth surfaces. The roughness is caused by the presence of the pores and by the roughness of the polymer, so the drop is in contact with both the rough polymer surface and air cavities. For these systems, the contact angle is always larger than that for a smooth surface (20). For example, the advancing contact angle of distilled water on a smooth PTFE surface reported in the literature varied from 108° to 112° (19), whereas in this work the contact angle reached a value of 123°, which is in agreement with the previous assessment.

4.3. Determination of r_{max} and γ_L^w from LEP-γ_L Curves

In order to plot LEP versus liquid surface tension, the dependence of surface tension on alcohol concentration in aqueous solutions must be known. Liquid surface tension data as a function of alcohol concentration at different temperatures were found in the literature. For aqueous solutions of methanol, ethanol, or isopropanol these data were taken from (21), and for aqueous *tert*-buthanol solutions they were taken from (22). All the data were fitted, for each alcohol and temperature, to the empirical equation (21),

$$\gamma_L = \gamma_W - (\gamma_W - \gamma_A)\frac{1 + ax_2}{1 - bx_2}x_1, \qquad [12]$$

where γ_L, γ_W, and γ_A are the surface tension of the liquid solution, distilled water, and alcohol, respectively, x_1 and x_2 are the molar fraction of alcohol and water, respectively, and a and b are the fitting parameters.

An example of LEP versus liquid surface tension plots at different temperatures is shown in Fig. 11. The experimental data recede below the linear regression line (solid line) for low alcohol concentrations and for distilled water, which correspond to higher surface tensions. This behavior is in agreement with Section 2 since the alcohols are polar liquids. So, the ranges of alcohol concentration for different alcohols where γ_L^d remains practically constant must be known in order to use Eq. [9]. The

TABLE 3
Contact Angles (in Sexagesimal Degrees) for Different Membranes at $t \cong 25°C$

Membrane	Liquid	Alcohol concentration (wt%)	θ (°)
PVDF22	Distilled water	—	110 (±3)
	Methanol–water	26.0	93 (±2)
		29.6	85 (±3)
	Ethanol–water	16.9	92 (±1)
		19.6	85 (±2)
	Isopropanol–water	10.4	94 (±1)
		13.1	70 (±2)
PVDF45	Distilled water	—	112 (±2)
	Ethanol–water	19.6	90 (±2)
	Isopropanol–water	10.4	99 (±1)
		14.0	90 (±2)
PTFE20	Distilled water	—	123 (±2)
	Methanol–water	87.4	94 (±5)
		88.1	92 (±5)
		89.1	87 (±4)
	Ethanol–water	70.9	93 (±2)
		72.7	87 (±2)
	Isopropanol–water	24.0	98 (±1)
		48.1	93 (±2)
		67.6	42 (±2)
	Tertbuthanol–water	16.7	91 (±3)
PTFE45	Distilled water	—	122 (±1)
	Isopropanol–water	35.0	99 (±3)
		40.8	81 (±6)
PTFS20	Distilled water	—	123 (±1)
	Isopropanol–water	29.0	94 (±3)
		37.8	78 (±5)

Note. Pure water and aqueous alcohol solutions at different concentrations of alcohol. The estimated standard errors are indicated in brackets.

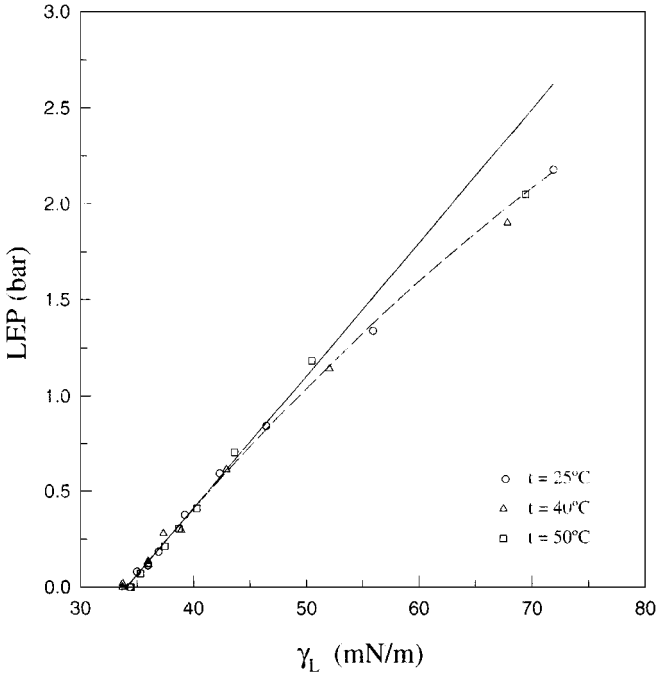

FIG. 11. LEP versus surface tension for isopropanol aqueous solutions at different temperatures. PVDF22 membranes. The solid line is the linear fit of the experimental data to Eq. [9] and the dashed line is shown as a visual guide.

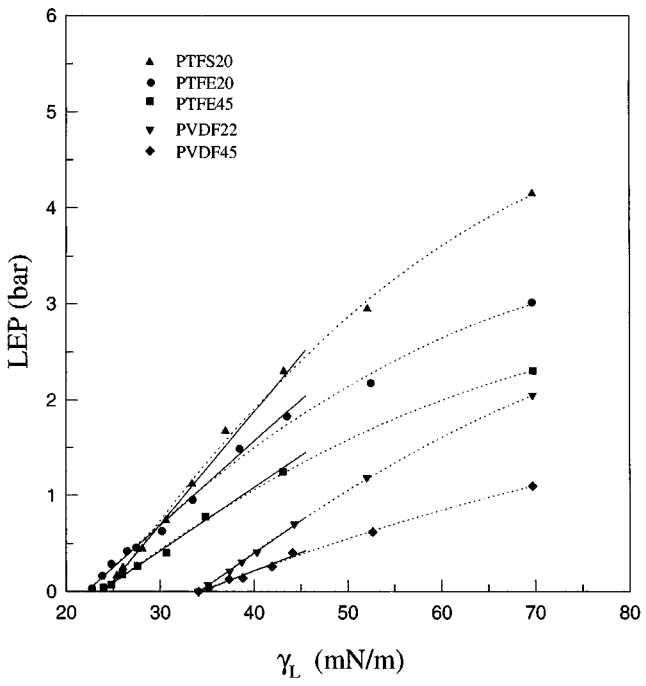

FIG. 12. LEP versus surface tension of isopropanol aqueous solutions for different membranes at $t = 40°C$. Solid lines are the linear fits of the experimental data to Eq. [9] and dashed lines are shown as a visual guide.

γ_L^d values were taken from (18) for the different alcohols used in this work, except for the case of *tert*-buthanol because for this alcohol γ_L^d values were not found. Note that it was not possible to take the dispersion component of the surface tension and the liquid surface tension data from the same reference because the dispersion component data were found at 20°C only (18). The alcohol concentration ranges from which γ_L^d can be supposed practically constant were estimated as follows: greater than 50% by weight for aqueous methanol solution, greater than 20% by weight for aqueous ethanol solution, and greater than 6% by weight for aqueous isopropanol solution. For the case of aqueous *tert*-buthanol solution, this range was directly estimated from the plots of LEP versus γ_L to be greater than 2% by weight. Characteristic membrane parameters, r_{max} and γ_L^w, will be estimated from linear fits to LEP-γ_L plots in those ranges.

Effect of membrane type on the curves of LEP versus γ_L is shown in Fig. 12. The data were fitted to Eq. [9] within the corresponding ranges of alcohol concentration. Again, a discrepancy between the linear regression line and the experimental points was observed for low concentrations (which correspond to higher surface tensions). This behavior has been observed in all the studied cases. Membrane parameters, r_{max} and γ_L^w, estimated from the linear fit are summarized in Table 4 for the different membranes, temperatures, and alcohols. The data listed in Table 4 indicate that there is not a clear dependence of the maximum pore radius on the type of alcohol. These results suggest that the molecule size, for the case of alcohols, does not influence on the determination of the maximum pore radius. The mean values of the maximum pore radius are 0.26 μm for

TABLE 4

Membrane Parameters Obtained from the Linear Fit of the Curves of LEP versus γ_L, within the Range of Concentration Where γ_L^d Remained Constant, for Different Membranes, Alcohols, and Temperatures

Membrane	Alcohol	t (°C)	r_{max} (μm)	γ_L^w (mN/m)
PVDF22	Methanol	40	0.224 (±0.013)	37 (±4)
	Ethanol	20	0.247 (±0.008)	36 (±2)
		40	0.223 (±0.007)	33 (±2)
	Isopropanol	20	0.245 (±0.012)	35 (±3)
		25	0.268 (±0.008)	34 (±2)
		40	0.287 (±0.008)	34 (±2)
		50	0.31 (±0.02)	34 (±5)
PVDF45	Ethanol	20	0.49 (±0.03)	35 (±4)
	Isopropanol	20	0.47 (±0.03)	34 (±5)
		40	0.51 (±0.04)	33 (±6)
PTFE20	Methanol	25	0.17 (±0.02)	23 (±6)
		40	0.18 (±0.02)	22 (±5)
	Ethanol	25	0.171 (±0.010)	24 (±3)
		40	0.172 (±0.013)	22 (±3)
	Isopropanol	25	0.208 (±0.013)	24 (±3)
		40	0.223 (±0.009)	22 (±2)
	Tert-butanol	25	0.135 (±0.009)	26 (±4)
		40	0.146 (±0.009)	26 (±4)
PTFE45	Isopropanol	40	0.317 (±0.011)	24 (±2)
PTFS20	Isopropanol	25	0.174 (±0.012)	24 (±2)
		40	0.185 (±0.008)	26 (±2)

Note. The estimated standard errors are indicated in brackets.

the PVDF22 membrane, 0.49 μm for the PVDF45 membrane, 0.18 μm for the PTFE20 membrane, 0.32 μm for the PTFE45 membrane, and 0.18 μm for the PTFS20 membrane. However, it seems that there is an increase of the maximum pore radius as the temperature increases, although this possible trend is disguised within the estimated standard error of the maximum pore radius. This trend could be explained if it is supposed that the polymeric material is contracted with increasing temperature. So, the membrane pore could become larger and a significant increase of the maximum liquid permeability, p_{max}, would be expected. In fact, in other experiments which do not appear in this work, the values of p_{max} for PTFE20 membranes were estimated to be 0.0622 ± 0.0007 and 0.086 ± 0.002 g cm^{-2} s^{-1} bar^{-1} at 25 and 40°C, respectively, using an aqueous solution of 9 wt% isopropanol.

Regarding the wetting surface tension, it seems to be independent of the type of alcohol used and the temperature. A similar trend has been already reported by van Giessen *et al.* (23), who noticed that in experiments with some low-energy solid surfaces, the contact angle of a drop seemed to depend almost entirely on the liquid–vapor surface tension and very little on the other properties of the liquid. The wetting surface tension was defined as the value of the surface tension when LEP is equal to zero, i.e., when the effective contact angle is 90°. Therefore, the wetting surface tension will depend very little on the type of liquid. Furthermore, if the standard errors are taken into account, the wetting surface tensions seem to agree to a similar value for each type of membrane, independently of the membrane pore size. The mean wetting surface tensions obtained in this work (i.e., $\gamma_L^w = 34$ mN/m for the PVDF membranes and $\gamma_L^w = 24$ mN/m for the PTFE membranes) are in good agreement with those reported in the literature (the γ_L^w values for the PVDF membranes varied from 34.2 mN/m (1) to 42.4 mN/m (8), and the γ_L^w values for the PTFE membrane varied from 24.2 mN/m (8) to 25.3 mN/m (3) for aqueous ethanol solutions and $\gamma_L^w >$ 22.8 mN/m (3) for aqueous isopropanol solutions).

4.4. *Determination of r_{max}, R/r and α_{max} from LEP, γ_L, and θ_A Data*

Values of r_{max} and R/r were estimated by using the measured values of contact angle and their corresponding liquid entry pressures for different alcohols. PTFE20 and PVDF22 membranes were used. Two data processings were carried out in order to determine the value of these characteristic membrane parameters: (a) via nonlinear fit to Eq. [4] using experimental values of LEP, γ_L, and θ_A, and (b) with the aid of a computer program by minimizing the deviation,

$$\chi^2 = \frac{1}{n}\sum_{i=1}^{n}\frac{\left(\mathrm{LEP}_{\mathrm{calc}_i} - \mathrm{LEP}_{\mathrm{exp}_i}\right)^2}{\mathrm{LEP}^2_{\mathrm{exp}_i}}, \qquad [13]$$

where LEP_{calc} is the liquid entry pressure calculated from Eq. [4] for each γ_L and θ_A value, LEP_{exp} is the experimental liquid entry pressure, and n is the number of measurements. Values of r_{max} and R/r were determined varying between 0.1 and 0.5 for the r_{max} parameter, and between 1 and 50 for the R/r parameter, until the smallest value of the function χ^2 was obtained.

TABLE 5
Characteristic Parameters of the Membrane Obtained from Different Fit Methods for PVDF22 and PTFE20 Membranes

Membrane	r_{max} (μm)	R/r	α_{max}	Fit method
PVDF22	0.251 (±0.014)	33 (±9)	−17°	*a*
	0.36 ±0.02[a]	18 ±2[a]	−23°	*b*
	0.26 (±0.03)	—	—	*c*
PTFE20	0.226 (±0.004)	48 (±10)	−14°	*a*
	0.33 ±0.01[a]	35 ±3[a]	−13°	*b*
	0.18 (±0.03)	—	—	*c*

Note. Fit method: *a*, Nonlinear fit; *b*, minimizing the function χ^2; *c*, linear fit of the curves of LEP versus γ_L. The estimated standard errors are indicated in brackets.

[a] Estimated errors.

Characteristic membrane parameters, r_{max} and R/r, estimated using the above two ways as well as maximum pore radius values obtained in Section 4.3 using linear fit to Eq. [9] are listed in Table 5. It is noticeable that the characteristic membrane parameters obtained from each data processing differ for the same membrane. The χ^2 method gives significantly larger values of r_{max} than the other methods. The closest comparison is obtained between the value of r_{max} estimated from the linear fit to Eq. [9] and that from the nonlinear fit to Eq. [4]. On the contrary, the values of R/r estimated from the χ^2 method are smaller than those estimated by means of the nonlinear fit to Eq. [4]. These trends were seen for both membranes. In addition, it is interesting to note that variations of R/r about 100% have no effect practically on the value of r_{max}. It must also be pointed out that the values of R/r estimated in this work are substantially larger than those reported in the literature ($R/r = 5.9$ for the PVDF45 membrane (1) or ranging from 2 to 10 for PTFE membranes (13)).

The nonlinear fit to Eq. [4] was satisfactory with a correlation coefficient adjusted to the degrees of freedom for the PVDF22 membrane of 0.983 for 7 points, and for the PTFE20 membrane of 0.996 for 10 points. Experimental liquid entry pressures as functions of those calculated for PVDF22 and PTFE20 membranes are shown in Fig. 13. The liquid entry pressures were calculated using the membrane parameters estimated from the nonlinear fit to Eq. [4]. The points depicted in Fig. 13 seem to follow the bisector of the coordinates' axes quite well. It is worth noting that the difference ($\mathrm{LEP}_{\mathrm{calc}_i} - \mathrm{LEP}_{\mathrm{exp}_i}$) calculated with the χ^2 method was greater than ($\mathrm{LEP}_{\mathrm{calc}_i} - \mathrm{LEP}_{\mathrm{exp}_i}$) calculated from the nonlinear fit to Eq. [4]. By using the values of r_{max} and R/r obtained from the χ^2 method, this difference with respect to $\mathrm{LEP}_{\mathrm{exp}_i}$ value was estimated to be 21% for PVDF22 membrane, and 26% for PTFE20 membrane against 5 and 13%, respectively, estimated by using the values of r_{max}, and R/r obtained from the nonlinear fit to Eq. [4].

Finally, the maximum structure angle, α_{max}, can be estimated by substituting r_{max} and R/r values into Eq. [2]. It should be

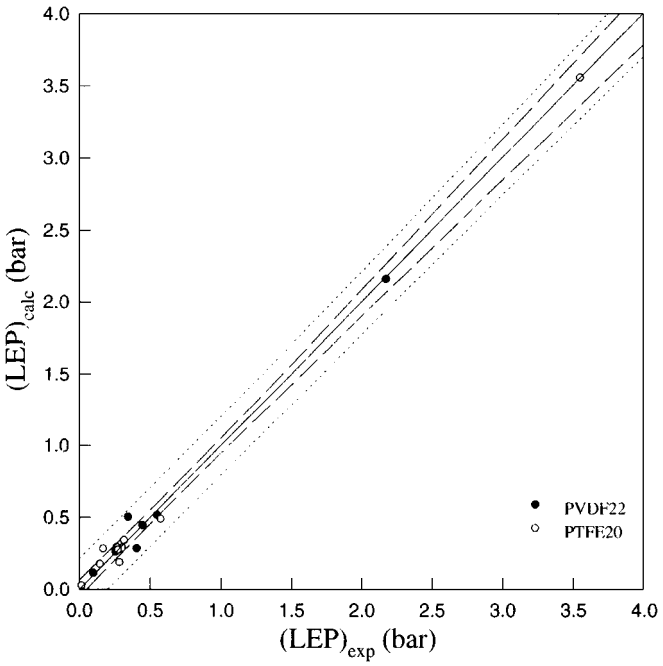

FIG. 13. Comparison of the values of LEP calculated from the nonlinear fits to Eq. [4] with the experimentally measured values. The solid line is the straight line with slope equal to 1, the dashed lines are the 95% confidence interval, and the dotted lines are the 95% prediction interval.

noted that the structure angle reaches its maximum value when the advancing contact angle is small. Therefore, aqueous solutions with alcohol concentration close to the wetting alcohol concentration have been chosen in order to estimate α_{max}. The maximum structure angles estimated using both data processings are also listed in Table 5 for PTFE20 and PVDF22 membranes. The LEP value is zero when $\theta_{ef} = \theta_A - \alpha = 90^\circ$, and so the liquid penetrates spontaneously into the membrane pores. A value of $\alpha_{max} = -17^\circ$ was estimated for the PVDF22 membrane by using the membrane parameters obtained from nonlinear fit, and a value of $\alpha_{max} = -23^\circ$ was estimated by using the membrane parameters obtained from the χ^2 method. Therefore, liquids whose advancing contact angles are less than or equal to 73° would penetrate spontaneously into the membrane pores. Taking into account the experimental values of LEP and those of contact angle, aqueous alcohol solutions whose contact angles are near 70° will penetrate spontaneously into the membrane pores. This result is in agreement with the values of α_{max} obtained from both methods. However, this estimation could not be carried out for the PTFE20 membrane because the values of contact angle obtained in this work for this membrane were not measured for alcohol concentrations sufficiently close to the wetting alcohol concentration.

5. CONCLUSIONS

The results of the liquid entry pressure measurements carried out herein were used to study its dependence on the process parameters (type of membrane, temperature, type of alcohol, and alcohol concentration), which are greatly important in membrane distillation processes. It was observed that the liquid entry pressure is strongly dependent on the alcohol concentration of aqueous solution, on the type of alcohol used, and on the temperature. It is worth noting that the discrepancy between the theoretical linear regression and the experimental liquid entry pressure data for low alcohol concentrations and distilled water confirms that the liquid entry pressure is affected by the dispersion component of surface tension of the solution, γ_L^d, which varies with alcohol concentration, even though the value of liquid–vapor surface tension was dominant in these experiments. Therefore, a linear relationship between the LEP value and its corresponding liquid surface tension, γ_L, was observed only within the range of alcohol concentration where γ_L^d remained practically constant.

The wetting surface tensions seem to be independent both of the type of alcohol used and the temperature; moreover, a similar value of γ_L^w was found for each type of membrane irrespective of the membrane pore radius. This result suggests to us that there is a unique wetting surface tension for each type of membrane, and so it would be enough to know the value of γ_L^w for one solution in order to be able to predict roughly the wetting concentration of any other solution on hydrophobic microporous membranes. The characteristic membrane parameters, r_{max}, R/r, and α_{max}, obtained from each data processing differed for the same membrane. Despite this, Eq. [4] was found suitable at least qualitatively for the determination of characteristic membrane parameters.

Finally, it may also be mentioned that all the experimental data as well as liquid surface tensions taken from the literature have been obtained from static methods. The characteristic membrane parameters cannot fulfill the requirements for membrane characterization in membrane processes, such as membrane distillation, since these values could not be extrapolated to dynamical processes, even though they could be valid as a maximum value of concentration for operating conditions. In membrane distillation processes, it is observed that maximum alcohol concentrations decreased by 15–20% with respect to predicted ones with LEP values at the same temperature, pressure difference, alcohol concentration, and membrane type.

ACKNOWLEDGMENTS

The authors gratefully acknowledge Professor J. Morales-Bruque at Extremadura University (Spain), who provided the facilities and helped carry out the contact angle measurements. The authors also thank CICYT (Spain), Projects ALI-94-1044-CO3-02 and PB98-0788, for financial support.

REFERENCES

1. Franken, A. C. M., Nolten, J. A. M., Mulder, M. H. V., Bargeman, D., and Smolders, C. A., *J. Membr. Sci.* **33,** 315 (1987).
2. Gekas, V., Persson, K. M., Wahlgren, M., and Sivik, B., *J. Membr. Sci.* **72,** 293 (1992).
3. Durham, R. J., and Nguyen, M. H., *J. Membr. Sci.* **87,** 181 (1994).

4. Izquierdo-Gil, M. A., García-Payo, M. C., and Fernández-Pineda, C., *J. Membr. Sci.* **155,** 45 (1999).
5. Izquierdo-Gil, M. A., García-Payo, M. C., and Fernández-Pineda, C., *Sep. Sci. Technol.* **34**(9), 1773 (1999).
6. Nakao, S., *J. Membr. Sci.* **96,** 131 (1994).
7. Kim, K. J., Fane, A. G., Ben Aim, R., Liu, M. G., Jonsson, G., Tessaro, I. C., Broek, A. P., and Bargeman, D., *J. Membr. Sci.* **87,** 35 (1994).
8. Keurentjes, J. T. F., Harbrecht, J. G., Brinkman, D., Hanemaaijer, J. H., Cohen Stuart, M. A., and van't Riet, K., *J. Membr. Sci.* **47,** 333 (1989).
9. McGuire, K. S., Lawson, K. W., and Lloyd, D. R., *J. Membr. Sci.* **99,** 127 (1995).
10. Lee, Y., Jeong, J., Youn, I. J., and Lee, W. H., *J. Membr. Sci.* **130,** 149 (1997).
11. Smolders, K., and Franken, A. C. M., *Desalination* **72,** 249 (1989).
12. García-Payo, M. C., Izquierdo-Gil, M. A., and Fernández-Pineda, C., *J. Membr. Sci.* **169,** 61 (2000).
13. Kim, B., and Harriott, P., *J. Colloid Interface Sci.* **115,** 1 (1987).
14. Zha, F. F., Fane, A. G., Fell, C. J. D., and Schofield, R. W., *J. Membr. Sci.* **75,** 69 (1992).
15. Lucassen-Reynders, E. H., *J. Phys. Chem.* **67,** 969 (1963).
16. Bargeman, D., *J. Colloid Interface Sci.* **40,** 344 (1972).
17. Dann, J. R., *J. Colloid Interface Sci.* **32,** 302 (1970).
18. Jańczuk, B., Białopiotrowicz, T., and Wójcik, W., *Colloids Surf.* **36,** 391 (1989).
19. Drelich, J., Miller, J. D., and Good, R. J., *J. Colloid Interface Sci.* **179,** 37 (1996).
20. Tröger, J., Lunkwitz, K., and Bürger, W., *J. Colloid Interface Sci.* **194,** 281 (1997).
21. Vázquez, G., Álvarez, E., and Navaza, J. M., *J. Chem. Eng. Data* **40,** 611 (1995).
22. Gliński, J., Chavepeyer, G., and Platten, J. K., *J. Chem. Phys.* **102,** 2113 (1995).
23. van Giessen, A. E., Bukman, D. J., and Widom, B., *J. Colloid Interface Sci.* **192,** 257 (1997).